PHYSICAL REVIEW D VOLUME 42, NUMBER 5 1 SEPTEMBER 1990

Generalized resonating-group-method equations in a $^3P_0$ $q\bar{q}$ condensed vacuum. The ϕ and ρ resonances

Pedro J. de A. Bicudo and José E. F. T. Ribeiro
Centro de Física da Matéria Condensada, Av. Prof. Gama Pinto 2, 1699 Lisboa, Portugal
(Received 2 August 1989)

The coupling of the bare resonances to the decay channels is implemented. We solve the Dyson series for the S matrix. The S matrix is cast in a separable expansion that leads to the resonating-group-method equations for the scattering. The overlap potential is shown to depend strongly on the cluster sizes. This strong dependence is reflected in the corresponding shift of the imaginary part of the resonance mass (the width of the resonance). Scattering amplitudes for K^+K^- ($\pi^+\pi^0$) close to the energy of ϕ (ρ^+) are also obtained. The results of this work are quite encouraging. The sensitivity of the scattering amplitudes to the cluster sizes (and to the chiral angle), and the strong restrictions to the possible values for the current quark masses and potential strength, lend a special role to the calculations of Argand plots, when measuring the extent of chiral-symmetry breaking in hadron physics.

I. INTRODUCTION

Hadron spectroscopy plays a central role in theoretical physics. In the last 15 years, theoretical approaches based on QCD furnished us, in the domain of high energy, high P_T, with a wealth of information about hadron structure.

On the other side of the energy domain, and despite the huge effort made in the last 50 years, it still can be said that we lack a quantitative, theoretically predicted explanation for the origin of the N-N forces, as well as the knowledge as to what extent nucleons can be usefully used as the essential building blocks of nuclei. Things only get more difficult if we look to describe, within the same framework, reactions such as N-$\bar{N}$ scattering. As is well known, the essential difficulty lies in the non-Abelian nature of QCD. But this is not the only difficulty. Even if we replace, somehow, gluon physics by some given quark-quark (antiquark) potential, the Dirac nature of the quarks will pose formidable problems when solving for the Hamiltonian spectrum. The study of these problems comes in the name of chiral physics. For instance and as we have seen, vacuum condensation is likely to occur. This condensation, being a strong event, will have a strong effect on hadronic phenomenology. The aim of this paper is precisely to study these effects in quantities such as mesonic masses and decay rates. These quantities will be shown to depend quite significantly on the extent of vacuum $^3P_0$, quark-antiquark condensation. Also, because of the relativistic nature of the light quarks u and d, the mesonic wave functions behave as a two-component "spinor" in an abstract "energy-spin" space. This will entail quite specific normalizations, in which the components can be quite large in some cases, for these wave functions. This fact introduces, per se, an essential departure from the usual nonrelativistic quark model.

In the present work we choose to work with a simple chirally invariant confining potential, the harmonic potential, partly due to the existence of some work done with this potential,[1] and partly because it allows algebraic simplifications to be made. Introducing a more realistic potential will only make actual calculations more cumbersome but will not change the physics involved. Another simplifying feature of the potential lies in it being instantaneous. Again, introducing retardation will add enormously to the extent and difficulty of the calculations, without modifying qualitatively, one hopes, the essential features introduced by the vacuum condensation. Throughout this work it is assumed that only quark-antiquark color singlets exist.

This paper is organized as follows. In Sec. II we discuss the Dyson equation for one and two quark-antiquark pairs, together with respective S matrices. Section III is devoted to the setting up of the associated resonating-group-method (RGM) equations. In Sec. IV we discuss the S- and T-matrix formalism for mesons with a separable potential. In Sec. V we evaluate the diagrams responsible for the overlap of a pair of mesons into a resonance, whereas the actual evaluation of the Green's functions, useful when dealing with the S and T formalism of Sec. IV is done in Sec. VI. Finally, results for the p-wave scatterings K^+K^- and $\pi^+\pi^-$, together with the conclusions are presented in Sec. VII.

II. DYSON EQUATIONS FOR 1 AND 2 MESONIC $q\bar{q}$ PAIRS

With our instantaneous interaction[2] we have for one meson[3] the diagrams of Fig. 1, whereas for two mesons we have to consider, in addition to the previous diagrams (this is mandatory, whenever one has annihilation or creation of quark-antiquark pairs) the exchange diagrams of Fig. 2, together with the interactions in Fig. 3, and finally when considering the coupling between one meson and two mesons, besides the aforementioned diagrams, the diagrams of Fig. 4 must also be considered.

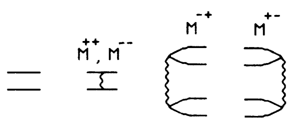

FIG. 1. Irreducible building blocks for one meson.

We shall describe the mesonic bound states with the help of the Dyson series for the S (and T) matrix. Later, mesons will be obtained as solutions of the homogeneous Dyson equations or, equivalently, as poles in the series.

For the sake of clarity we shall proceed in steps. First we will consider mesons having no negative-energy terms (i.e., without the annihilation of two $q\bar{q}$ pairs) and without exchange. Second the negative-energy diagrams will be introduced. After this, we will deal with quark exchange but without negative energies and, finally, exchange and negative-energy diagrams will be considered simultaneously.

All these cases correspond to physical situations (for instance, in many elastic scattering processes, flavor conservation forbids exchange). As for the negative-energy terms, they are a consequence of how relativistic the reaction under consideration is, and they vanish for heavy mesons.

A. Mesons without negative energy or exchange

This is the case for bottomonium states and for their strong decay products, and to a lesser extent for charmonium. If we have only one meson, we obtain the Dyson series of Fig. 5. When summing the diagrams in the Dyson series one must be careful to avoid double counting. In Fig. 5 we denote the product of quark and antiquark propagators as

$$G = G_{0q_1} G_{0\bar{q}_2} \ . \tag{2.1}$$

Defining the integral operator M as

$$M = G \int \frac{d^3k\, dw}{(2\pi)^4} V_{q_1\bar{q}_2} \ , \tag{2.2}$$

then the Dyson series for the S matrix is given by

$$S_M = G + MG + M^2G + M^3G + \cdots \ . \tag{2.3}$$

This satisfies the Dyson equation

$$S_M = G + MS_M \tag{2.4}$$

with the solution

$$S_M = \frac{1}{1-M} G \ . \tag{2.5}$$

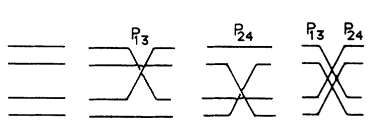

FIG. 2. Quark and antiquark exchange diagrams.

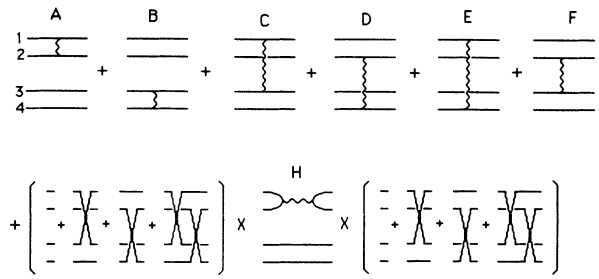

FIG. 3. Intra and intercluster interactions.

If we have two mesons but no exchange, only the intercluster diagrams A and B are to be used in the series. Without quark exchange the other diagrams C–F do not contribute between a pair of color singlets. This is clearly seen in Fig. 6. In this case the S matrix looks like Fig. 7, where we denote the product of the four quark and antiquark propagators as

$$G = G_{0q_1} G_{0\bar{q}_2} G_{0q_3} G_{0\bar{q}_4} \tag{2.6}$$

and define the integral operators A and B as

$$A = G \int \frac{d^3k\, dw}{(2\pi)^4} V_{q_1\bar{q}_2}, \quad B = G \int \frac{d^3k\, dw}{(2\pi)^4} V_{q_3\bar{q}_4} \ . \tag{2.7}$$

In this case, the Dyson series for the S matrix reads

$$\begin{aligned} S_{AB} = {} & G + AG + BG + A^2G + ABG + B^2G \\ & + A^3G + A^2BG \\ & + AB^2G + B^3G + \cdots \ , \end{aligned} \tag{2.8}$$

where A and B commute. We must be careful because AB and BA correspond to the same diagram. They may not be repeated otherwise we would have the duplication of terms. The series (2.8) can be factorized:

$$S_{AB} = (1 + A + A^2 + A^3 + \cdots)(1 + B + B^2 + B^3 + \cdots)G \tag{2.9}$$

and summed to give

$$S_{AB} = S_A \otimes S_B = \frac{1}{(1-A)(1-B)} G \ . \tag{2.10}$$

S_{AB} satisfies the equation

$$S_{AB} = G + [1 - (1-A)(1-B)] S_{AB} \ . \tag{2.11}$$

This result can be generalized to any set of commuting interactions. The Dyson equation for the S matrix is

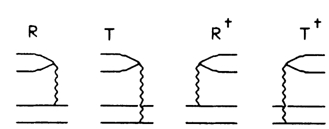

FIG. 4. Interactions responsible for the annihilation and creation of a quark and antiquark pair.

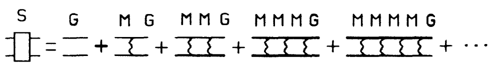

FIG. 5. Dyson series for the S matrix for one meson (quark-antiquark scattering) in the ladder approximation.

therefore

$$S_{AB}=G+(A+B-AB)S_{AB}\ , \tag{2.12}$$

where the term $-AB$ removes the double counting of diagrams.

If we have a coupling between channels of one and two mesons, starting from Eqs. (2.4) and (2.11) already obtained,

$$\begin{aligned} &S_1=G_1+V_1S_1, \quad V_1=M\ ,\\ &S_2=G_2+V_2S_2, \quad V_2=A+B-AB\ , \end{aligned} \tag{2.13}$$

and using the potentials

$$\begin{aligned} &V_{12}=G_1\int(R^\dagger+T^\dagger)(P_{13}+P_{24})\ ,\\ &V_{21}=G_2(P_{13}+P_{24})\int R+T\ , \end{aligned} \tag{2.14}$$

which induce the transition from channel one to channel two and vice versa (the exchange of the created or annihilated quark or antiquark is necessary if we want to obtain a pair of mesons behaving as color singlets), we are able to define four different S matrices coupling the two different channels. They can be obtained (without double counting) with the help of the series

$$\begin{aligned} S_{11}&=S_1+(S_1G_1^{-1})V_{12}(S_2G_2^{-1})V_{21}S_{11}\\ &=\frac{1}{1-(S_1G_1^{-1})V_{12}(S_2G_2^{-1})V_{21}}S_1\\ &=\frac{1}{1-V_1-V_{12}\dfrac{1}{1-V_2}V_{21}}G_1\ ,\\ S_{22}&=\frac{1}{1-V_2-V_{21}\dfrac{1}{1-V_1}V_{12}}G_2\ ,\\ S_{12}&=(S_{11}G_1^{-1})V_{12}S_2=(S_1G_1^{-1})V_{12}S_{22}\\ &=\frac{1}{-V_{21}+(1-V_2)\dfrac{1}{V_{12}}(1-V_1)}G_2\ , \end{aligned}$$

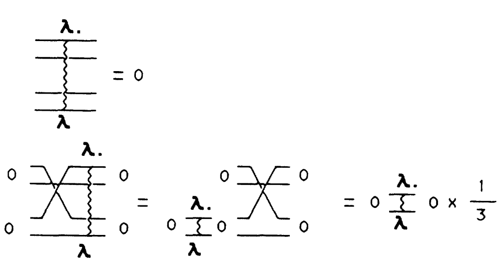

FIG. 6. Color algebra between singlets. The role of quark exchange.

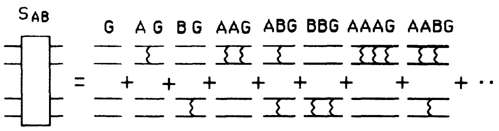

FIG. 7. Dyson series for the scattering of two noninteracting mesons, in the ladder approximation.

$$\begin{aligned} S_{21}&=(S_{22}G_2^{-1})V_{21}S_1=(S_2G_2^{-1})V_{21}S_{11}\\ &=\frac{1}{-V_{12}+(1-V_1)\dfrac{1}{V_{21}}(1-V_2)}G_1\ . \end{aligned} \tag{2.15}$$

These four equations can be cast in the form of a matrix equation:

$$[S]_{ij}=\left[\frac{\mathbb{1}}{\mathbb{1}-\begin{bmatrix}V_1 & V_{12}\\ V_{21} & V_2\end{bmatrix}}\right]_{ij}G_j \tag{2.16}$$

which is, in turn, a solution of the Dyson equation:

$$\begin{bmatrix}S_{11} & S_{12}\\ S_{21} & S_{22}\end{bmatrix}=\begin{bmatrix}G_1 & 0\\ 0 & G_2\end{bmatrix}+\begin{bmatrix}V_1 & V_{12}\\ V_{21} & V_2\end{bmatrix}\begin{bmatrix}S_{11} & S_{12}\\ S_{21} & S_{22}\end{bmatrix}\ . \tag{2.17}$$

Again, this result can be generalized to any number of coupled channels.

In fact, in Eq. (2.17) the columns of the S matrix are coupled separately and, therefore, the two homogeneous equations, one for each column, must be degenerate:

$$\begin{bmatrix}S_{1a}\\ S_{2a}\end{bmatrix}=\begin{bmatrix}V_1 & V_{12}\\ V_{21} & V_2\end{bmatrix}\begin{bmatrix}S_{1a}\\ S_{2a}\end{bmatrix},\quad a=1;2\ . \tag{2.18}$$

Had we used the V matrix acting on the right of the S matrix, then only the rows would be coupled. This implies that, in the neighborhood of a pole of S (precisely when the homogeneous equation has a solution), the S matrix takes the form of a tensor product:

$$S_{ab}=\phi_a\times\text{pole}\times\phi_b^\dagger\ . \tag{2.19}$$

B. Mesons with positive and negative energies

This is the case for the scattering of mesons in exotic channels. If we consider mesons without exchange but with negative-energy components then even for a single meson we obtain a coupled-channel equation, better known as the Bethe-Salpeter equation:[3]

$$\begin{bmatrix} S^{++} & S^{+-} \\ S^{-+} & S^{--} \end{bmatrix} = \begin{bmatrix} G^{+} & 0 \\ 0 & G^{-} \end{bmatrix} + \begin{bmatrix} M^{++} & M^{+-} \\ M^{-+} & M^{--} \end{bmatrix} \begin{bmatrix} S^{++} & S^{+-} \\ S^{-+} & S^{--} \end{bmatrix} . \tag{2.20}$$

As the case without negative energies, for two noninteracting mesons (exchange is not considered) the S matrix is given by the tensor product of two one-meson S matrices.

$$\begin{aligned} S_{AB} &= S_A \otimes S_B \\ &= G_A \otimes G_B + (A \otimes \mathbb{1} + \mathbb{1} \otimes B - A \otimes B) S_{AB} \end{aligned} \tag{2.21}$$

with the exception that it is now an equation for rank-4 matrices. The homogeneous equation then reads

$$\begin{bmatrix} A^{++}+B^{++}-A^{++}B^{++} & B^{+-}-A^{++}B^{+-} & A^{+-}-A^{+-}B^{++} & -A^{+-}B^{+-} \\ B^{-+}-A^{++}B^{-+} & A^{++}+B^{--}-A^{++}B^{--} & -A^{+-}B^{-+} & A^{+-}-A^{+-}B^{--} \\ A^{-+}-A^{-+}B^{++} & -A^{-+}B^{+-} & A^{--}+B^{++}-A^{--}B^{++} & B^{+-}-A^{--}B^{+-} \\ -A^{-+}B^{-+} & A^{-+}-A^{-+}B^{--} & B^{-+}-A^{--}B^{-+} & A^{--}+B^{--}-A^{--}B^{--} \end{bmatrix} \times \begin{bmatrix} S^{++;ab} \\ S^{+-;ab} \\ S^{-+;ab} \\ S^{--;ab} \end{bmatrix} = \begin{bmatrix} S^{++;ab} \\ S^{+-;ab} \\ S^{-+;ab} \\ S^{--;ab} \end{bmatrix} . \tag{2.22}$$

Whenever we couple a channel for one meson with a channel for two mesons then we have to deal with a rank-6 matrix. The form is the same as in the case without negative energies except that now V_2 is a 4×4 matrix and V_1 a 2×2 matrix. The coupling interaction V_{12} is a 4×2 matrix, and is given by

$$\begin{aligned} &V_{12}^{+;++} = G_1 \int (R^\dagger + T^\dagger)(P_{13}+P_{24}) , \\ &V_{12}^{+;-+} = V_{12}^{+;+-} = G_2(P_{13}+P_{24}) \int R + T , \\ &V_{12}^{+;--} = 0, \quad V_{12}^{-;++} = 0 , \\ &V_{12}^{-;+-} = G_2(P_{13}+P_{24}) \int R + T , \\ &V_{12}^{-;-+} = G_2(P_{13}+P_{24}) \int R + T , \\ &V_{12}^{-;--} = G_1 \int (R^\dagger + T^\dagger)(P_{13}+P_{24}) . \end{aligned} \tag{2.23}$$

C. Mesons with exchange

If we consider mesons where exchange is possible but still having no negative-energy amplitudes, there is no difference when considering one meson alone. However, in the channels with two mesons, diagrams C–F start to contribute (see Fig. 3). Diagrams H (see Fig. 3) also contribute. They correspond to an interaction between different mesons. The only diagrams which commute are now A with B, C with D, E with F, and also H with B.

We have already derived the Dyson equation for commuting diagrams. We shall now consider the case of two noncommuting diagrams, say, A and C. The complete Dyson series for the S matrix, without double counting, can be obtained as follows:

$$\begin{aligned} S_{AC} &= S_A + S_A G^{-1} C S_A + S_A G^{-1} C S_A G^{-1} C S_A + \cdots \\ &= S_A + S_A G^{-1} C S_{AC} . \end{aligned} \tag{2.24}$$

If we multiply Eq. (2.24) from the left with GS_A^{-1}, we obtain the equation

$$(GS_A^{-1} - C) S_{AC} = G \tag{2.25}$$

or

$$[1-(A+C)] S_{AC} = G . \tag{2.26}$$

Now consider the general problem where the Dyson equation is already known for a certain set of diagrams. If we introduce a new diagram A, we can decompose the previous set of diagrams of the Dyson equation in a sum, let us call it B, of diagrams commuting with A plus a sum of diagrams C that do not commute with A. The previous S matrix was

$$\begin{aligned} S_{BC} &= [1-(B+C)] S_{BC} \\ &= S_B + S_B G^{-1} C S_B + S_B G^{-1} C S_B G^{-1} C S_B + \cdots \end{aligned} \tag{2.27}$$

and the new one can be written as

$$\begin{aligned} S_{ABC} &= S_A \otimes S_B + S_A \otimes S_B G^{-1} C S_A \otimes S_B + \cdots \\ &= S_A \otimes S_B + S_A \otimes S_B G^{-1} C S_{ABC} . \end{aligned} \tag{2.28}$$

Then the corresponding Dyson equation looks like

$$[G(S_A \otimes S_B)^{-1} - C] S_{ABC} = G \tag{2.29}$$

or

$$[1-(A+B-AB+C)] S_{ABC} = G . \tag{2.30}$$

If we iterate Eq. (2.30), we find that in the general case without exchange, the coefficient of the Dyson equation for the S matrix is given by

1 − the sum of all irreducible diagrams

+ the sum of the product of all pairs of commuting irreducible diagrams

− the sum of all triplets of commuting irreducible diagrams + ⋯ . (2.31)

In many cases—including $\pi\pi$ scattering, which we will consider later—we have to consider the exchange of fermions. For our system of four fermions $q_1\bar{q}_2q_3\bar{q}_4$, the antisymmetrizer reads

$$\mathcal{A}=1-P_{13}-P_{24}+P_{13}P_{24} \ . \tag{2.32}$$

For the S matrix, in order to avoid double counting, we can slide all exchange diagrams to one side of the fermionic lines in the Dyson series. It is only in the case of the annihilation-creation diagram H that this sliding cannot be performed. We obtain the Dyson equation

$$[1-A-B+AB-C-D+CD-E-F+EF-\mathcal{A}(H-HB)]S=\mathcal{A}G \ . \tag{2.33}$$

Now if we consider the coupling of one channel for one meson with a channel for two mesons, we are naturally led to the equation:

$$\begin{bmatrix} 1-M & R^\dagger+T^\dagger \\ \mathcal{A}(R+T) & 1-A-B+AB-C-D+CD-E-F+EF-\mathcal{A}(H-HB) \end{bmatrix} \begin{bmatrix} S_{11} & S_{12} \\ S_{21} & S_{22} \end{bmatrix} = \begin{bmatrix} G_1 & 0 \\ 0 & \mathcal{A}G_2 \end{bmatrix} . \tag{2.34}$$

D. Mesons with exchange and with negative energies

This is a straightforward but cumbersome generalization of the two preceding cases.

III. GENERALIZED RGM EQUATIONS

The RGM equations[4] are the dynamical equations for coupled channels of bound states and resonances. In our case we want to integrate the explicit quark degrees of freedom to obtain the corresponding equations for mesons.

In this section it will be shown that the RGM equations are obtained simply by "replacing," in the Dyson equations for the S matrix, the corresponding solutions of the Bethe-Salpeter equations.

In our case, we recall that the vacuum is condensed into $^3P_0$ $q\bar{q}$ pairs, that the quarks are relativistic; and that mesons have positive and negative-energy wave functions. However we will show that the RGM equations are still Schrödinger-like equations for coupled channels (except for the kinetic energies which can be relativistic).

We note that this derivation of the RGM can be easily extended both in the direction of using bound states with more than one quark such as baryons (qqq bound states) and in the direction of using bound states of bound states (for instance, going to the nuclear level and so on. . .).

A. The S matrix for a channel of one meson

If we have a single $q\bar{q}$ pair, then the S matrix obeys the Dyson equation (or inhomogeneous Salpeter equation)

$$\begin{aligned} S^{++}&=G_0(+E)+S^{++}G_0^{-1}(+E)M^{++}G_0(+E) \\ &\quad +S^{+-}G_0^{-1}(-E)M^{-+}G_0(+E) \ , \\ S^{+-}&=0+S^{++}G_0^{-1}(+E)M^{+-}G_0(-E) \\ &\quad +S^{+-}G_0^{-1}(-E)M^{--}G_0(-E) \ . \end{aligned} \tag{3.1}$$

As usual, we define

$$M^{\alpha\beta}=G_0(\alpha E)\int V^{\alpha\beta} \ . \tag{3.2}$$

If we multiply, from the right, expressions (3.1) with $G_0^{-1}(+E)\phi^-$ and $G_0^{-1}(-E)\phi^-$, respectively, and add them, we are led to the expression

$$\begin{aligned} S^{++}G_0^{-1}(+E)\phi^+ +S^{+-}G_0^{-1}(-E)\phi^- &=\phi^+ +S^{++}G_0^{-1}(+E)M^{++}\phi^+ +S^{+-}G_0^{-1}(-E)M^{-+}\phi^+ \\ &\quad +S^{++}G_0^{-1}(+E)M^{+-}\phi^- +S^{+-}G_0^{-1}(-E)M^{--}\phi^- \ . \end{aligned} \tag{3.3}$$

We also know that on mass shell the wave functions are solutions of the homogeneous Salpeter equation

$$\begin{aligned} G_0^{-1}(+E_M)\phi^+&=\int V^{++}\phi^+ +\int V^{+-}\phi^- \ , \\ G_0^{-1}(-E_M)\phi^-&=\int V^{-+}\phi^+ +\int V^{--}\phi^- \ , \end{aligned} \tag{3.4}$$

where E_M is the on-shell energy of the meson M. Now, replacing these equations in expression (3.3) we get

$$\begin{aligned} S^{++}&[G_0^{-1}(+E)-G_0^{-1}(+E_M)]\phi^+ \\ &+S^{+-}[G_0^{-1}(-E)-G_0^{-1}(-E_M)]\phi^- =\phi^+ \ , \end{aligned} \tag{3.5}$$

where the Green's function for a quark-antiquark pair is (the relative energy has already been integrated out)

$$G_0(E,\mathbf{P},\mathbf{k})=\frac{i}{E-E_q(\mathbf{k}+\mathbf{P}/2)-E_{\bar{q}}(-\mathbf{k}+\mathbf{P}/2)+2i\epsilon} \ . \tag{3.6}$$

Thus in (3.5) the difference of inverse Green's functions does not depend on the quark energies and we obtain finally

$$S^{++}\phi^{+}-S^{+-}\phi^{-}=\phi^{+}\frac{i}{E-E_M} . \tag{3.7}$$

Had we started with the Salpeter equations for the other column (or for the lines of the S matrix), we would have obtained the equations

$$\begin{aligned} &S^{++}\phi^{+}-S^{+-}\phi^{-}=\phi^{+}\frac{i}{E-E_M} ,\\ &S^{-+}\phi^{+}-S^{--}\phi^{-}=\phi^{-}\frac{i}{E-E_M} ,\\ &\phi^{\dagger +}S^{++}-\phi^{\dagger -}S^{-+}=\frac{i}{E-E_M}\phi^{\dagger +} ,\\ &\phi^{\dagger +}S^{+-}-\phi^{\dagger -}S^{--}=\frac{i}{E-E_M}\phi^{\dagger -} . \end{aligned} \tag{3.8}$$

Now, if we normalize the wave functions with the integral condition

$$\int(\phi^{\dagger +}\phi^{+}-\phi^{\dagger -}\phi^{-})=1 \tag{3.9}$$

the solution of expressions (3.8) is

$$S^{\alpha\beta}(\mathbf{k},\mathbf{k}',E)=\phi^{\alpha}(\mathbf{k})\frac{i}{E-E_M+i\epsilon}\phi^{\dagger\beta}(\mathbf{k}') + \text{orthogonal terms} . \tag{3.10}$$

ϕ^{α} and ϕ^{β} above are solutions of the appropriate Salpeter equation for mesons. In (3.10) a factor $+i\epsilon$ was included since we want the meson to propagate forward in time.

The remaining orthogonal terms correspond to all other solutions of the Salpeter equation. Because the potential is confining, there are no solutions in the continuum for a pair of a quark and an antiquark, just bound states that we represent with a subscript c. Then the S matrix takes the separable form

$$S^{\alpha\beta}(\mathbf{k},\mathbf{k}',E)=\sum_c \phi_c^{\alpha}(\mathbf{k})\frac{i}{E-E_c+i\epsilon}\phi_c^{\dagger\beta}(\mathbf{k}') . \tag{3.11}$$

In the case where the mesons are heavy, it suffices to consider the positive-energy wave functions.

B. The S matrix for a channel of two mesons without quark exchange

Without quark exchange, the S matrix is just the product of two one-meson [see Eq. (2.21)] S matrices:

$$\begin{aligned} S_{AB}^{\alpha\beta\gamma\delta}&=S_A^{\alpha\beta}\otimes S_B^{\gamma\delta}\\ &=\sum_a \phi_a^{\alpha}(\mathbf{k})\frac{i}{E/2+W-E_a+i\epsilon}\phi_a^{\dagger\beta}(\mathbf{k}')\\ &\otimes\sum_b \phi_b^{\gamma}(\mathbf{k})\frac{i}{E/2-W-E_b+i\epsilon}\phi_b^{\dagger\delta}(\mathbf{k}') . \end{aligned} \tag{3.12}$$

It is a function only of the relative momentum of the $q\bar{q}$ pairs inside the mesons A and B. From the point of view of the relative and center-of-mass momenta for the mesons as a whole, it is a constant.

As the interactions are instantaneous, they do not depend on the energies. Then we will always integrate over the meson-meson relative energy W, in order to obtain a simpler propagator:

$$\int\frac{dW}{2\pi}\frac{i}{E/2+W-E_a+i\epsilon}\frac{i}{E/2-W-E_b+i\epsilon}=\frac{i}{E-E_a-E_b+i\epsilon} . \tag{3.13}$$

C. The S matrix for a channel of one meson coupled with a channel of two mesons still without quark exchange

We define S_1 and G_1 as pertaining to the channel (of one meson) and S_2 and G_2 for the corresponding quantities in channel two (of two mesons). We also define the transition potentials V_{12} and V_{21} as [see Eq. (2.23)]

$$\begin{aligned} V_{12}&=G_1\int V_{12,\text{truncated}} ,\\ V_{21}&=G_2\int V_{21,\text{truncated}} . \end{aligned} \tag{3.14}$$

Then the S matrix for the different channels, given by Dyson series, obeys the following equations [see Eq. (2.15)]:

$$\begin{aligned} S_{11}&=S_1+(S_1G_1^{-1})V_{12}(S_2G_2^{-1})V_{21}S_{11} ,\\ S_{22}&=S_2+(S_2G_2^{-1})V_{21}(S_1G_1^{-1})V_{12}S_{22} ,\\ S_{12}&=(S_{11}G_1^{-1})V_{12}S_2=(S_1G_1^{-1})V_{12}S_{22} ,\\ S_{21}&=(S_{22}G_2^{-1})V_{21}S_1=(S_2G_2^{-1})V_{21}S_{11} , \end{aligned} \tag{3.15}$$

where both the one-channel and the coupled-channel S_{ij} matrix elements are in turn matrices because they contain all the positive- and negative-energy terms. In the above equations we can replace S_1 and S_2 by their separable expansions. In matrix notation we obtain, using the bra-ket formalism,

$$\begin{aligned} S_1^{\alpha\beta}&=\sum_{c=1}^{n_c}|\phi_c^{\alpha}\rangle\frac{i}{E-E_c+i\epsilon}\langle\phi_c^{\beta}| ,\\ S_2^{\alpha\beta\gamma\delta}&=\sum_{a=1,\ b=1}^{n_a,n_b}|\phi_a^{\alpha}\rangle|\phi_b^{\gamma}\rangle\frac{i}{E-E_a-E_b+i\epsilon}\langle\phi_a^{\beta}|\langle\phi_b^{\delta}| . \end{aligned} \tag{3.16}$$

In practice we approximate S by truncating this expansion to a finite number (n_a, n_b, and n_c) of bound states. In a matrix notation for the indices a,b,c and α,β,γ we obtain

$$\begin{aligned} S_{11}=|\phi_1\rangle\frac{i}{E-E_c}\langle\phi_1|+|\phi_1\rangle &\times\frac{i}{E-E_c}\langle\phi_1|V_{12,\ \text{truncated}}|\phi_A\rangle|\phi_B\rangle\\ &\times\frac{i}{E-E_a-E_b}\langle\phi_A|\langle\phi_B|V_{21,\ \text{truncated}}S_{11} . \end{aligned} \tag{3.17}$$

It suffices to iterate this relation, to see that the S_{11} matrix, as S_1, is of the separable form

$$S_{11}^{\alpha\beta}=\sum_{c=1}^{n_c}|\phi_c^{\alpha}\rangle s_{11}\langle\phi_c^{\beta}| , \tag{3.18}$$

where s_{11} turns out to be a c number in the space of the bound states. Expression (3.17) then becomes

$$|\phi_1\rangle s_{11}\langle\phi_1| = |\phi_1\rangle \frac{i}{E-E_c}\langle\phi_1| + |\phi_1\rangle \frac{i}{E-E_c}\langle\phi_1|V_{12,\text{ truncated}}|\phi_A\rangle|\phi_B\rangle \times \frac{i}{E-E_a-E_b}\langle\phi_A|\langle\phi_B|V_{21,\text{ truncated}}|\phi_1\rangle s_{11}\langle\phi_1| \ . \tag{3.19}$$

In fact, because of the positive and negative energies, we have a system of $2n_c \times 2n_c$ equations. But if we factorize out the external $|\phi_c^\alpha\rangle$ and $\langle\phi_c^\beta|$, we see that the equations are all degenerate and can be cast in a smaller set of $n_c \times n_c$ equations; *this time for the small s matrix:*

$$s_{11} = g_1 + g_1\langle v_{12}|g_2|v_{21}\rangle s_{11} \ . \tag{3.20}$$

In (3.20) g_1 and g_2 are the one-meson and the two-meson propagators, respectively. $\langle v_{12}|$ and $|v_{21}\rangle$ (c numbers, respectively, to the left and right, and operators, acting on the relative momentum between mesons A and B, respectively, to the right and left) are the transition potentials:

$$\langle v_{12}|_{cab} = \sum_{\alpha\beta\gamma} \langle\phi_c^\alpha|V_{12,\text{ truncated}}|\phi_a^\beta\rangle|\phi_b^\gamma\rangle \ , \quad |v_{21}\rangle = \text{H.c.} \tag{3.21}$$

In the same way, for the channel 22 we obtain a system of $2n_a 2n_b \times 2n_a 2n_b$ equations:

$$S_{22} = |\phi_A\rangle|\phi_B\rangle \frac{i}{E-E_a-E_b}\langle\phi_A|\langle\phi_B| + |\phi_A\rangle|\phi_B\rangle \frac{i}{E-E_a-E_b} \times \langle\phi_A|\langle\phi_B|V_{21,\text{ truncated}}|\phi_1\rangle \frac{i}{E-E_c}\langle\phi_1|V_{12,\text{ truncated}}S_{22} \ , \tag{3.22}$$

where the S matrix S_{22} reads

$$S_{22}^{\alpha\beta\gamma\delta} = |\phi_a^\alpha\rangle|\phi_b^\beta\rangle s_{22}\langle\phi_a^\gamma|\langle\phi_b^\delta| \ . \tag{3.23}$$

In (3.23) s_2 is a q number on the relative momentum between the mesons A and B, and an $n_a n_b \times n_a n_b$ matrix in the space of bound states. The $2n_a 2n_b \times 2n_a 2n_b$ equations are degenerate and, again, if we factorize out the external bras and kets, we obtain the equation, *this time for small s,*

$$s_{22} = g_2 + g_2|v_{21}\rangle g_1\langle v_{12}|s_{22} \ . \tag{3.24}$$

Similarly, we have

$$S_{12}^{\alpha\gamma\delta} = |\phi_1^\alpha\rangle s_{12}\langle\phi_A^\gamma|\langle\phi_B^\delta| \ , \quad S_{21}^{\alpha\beta\gamma} = |\phi_A^\alpha\rangle|\phi_B^\beta\rangle s_{21}\langle\phi_1^\gamma| \ , \tag{3.25}$$

where s_{12} is an operator acting only to the right while s_{21} is operator acting only to the left. They also are matrices in the space of bound states of dimension $n_c \times n_a n_b$. They obey the equations

$$s_{12} = s_{11}\langle v_{12}|g_2 = g_1\langle v_{12}|s_{22} \ , \tag{3.26a}$$

$$s_{21} = s_{22}|v_{21}\rangle g_1 = g_2|v_{21}\rangle s_{11} \ . \tag{3.26b}$$

Now, exactly in the same way as we did for the S_{ij} that were *S matrices for the quarks,* we can obtain a matrix equation for the *mesonic* s_{ij}:

$$\begin{aligned} &(3.20),(3.26\text{a}) \Longrightarrow s_{11} - g_1\langle v_{12}|s_{21} = g_1 \ , \\ &(3.24),(3.26\text{b}) \Longrightarrow s_{22} - g_2|v_{21}\rangle s_{12} = g_2 \ , \\ &(3.26\text{a}) \Longrightarrow s_{12} - g_1\langle v_{12}|s_{22} = 0 \ , \\ &(3.26\text{b}) \Longrightarrow s_{21} - g_2|v_{21}\rangle s_{11} = 0 \end{aligned} \tag{3.27}$$

or, when written in matrix notation,

$$\begin{bmatrix} 1 & -g_1\langle v_{12}| \\ -g_1|v_{21}\rangle & 1 \end{bmatrix} \begin{bmatrix} s_{11} & s_{12} \\ s_{21} & s_{22} \end{bmatrix} = \begin{bmatrix} g_1 & 0 \\ 0 & g_2 \end{bmatrix} \ . \tag{3.28}$$

If we multiply (3.28) from the left by

$$\begin{bmatrix} ig_1^{-1} & 0 \\ 0 & ig_2^{-1} \end{bmatrix}$$

we obtain

$$\begin{bmatrix} E-E_c & -i\langle v_{12}| \\ -i|v_{21}\rangle & E-E_a-E_b \end{bmatrix} \begin{bmatrix} s_{11} & s_{12} \\ s_{21} & s_{22} \end{bmatrix} = \begin{bmatrix} i & 0 \\ 0 & i \end{bmatrix} , \tag{3.29}$$

where the $-i\langle v_{12}|$ is real because the potential already contains a factor $-i$ according to the Feynman rules.

In (3.29) the columns of s_{ij} are decoupled. Had we studied the equation with the operators on the left, then rows, instead of columns, would be decoupled. In this way, in the neighborhood of the pole we may write

$$\begin{aligned} &s_{11} = c_1 \times \text{pole} \times c_1, \quad s_{12} = c_1 \times \text{pole} \times \langle\chi_2| \ , \\ &s_{21} = |\chi_2\rangle \times \text{pole} \times c_1, \quad s_{22} = |\chi_2\rangle \times \text{pole} \times \langle\chi_2| \ . \end{aligned} \tag{3.30}$$

The RGM equation is the homogeneous equation (it is the same for the T matrix and for the S matrix) with the Schrödinger-like form:

$$\begin{bmatrix} E-E_c & -i\langle v_{12}| \\ -i|v_{21}\rangle & E-E_a-E_b \end{bmatrix} \begin{bmatrix} c_1 \\ |\chi_2\rangle \end{bmatrix} = 0 \ . \tag{3.31}$$

D. The s matrix with quark exchange and direct meson-meson interaction

In the present model, quark exchange and interaction between two different mesonic $q\bar{q}$ pairs should be considered in the Salpeter equation, as an interaction between the incoming and outgoing $q\bar{q}$ lines of the S matrix, in K^+-K^- scattering flavor conservation kills exchange contributions and only diagram H should be considered, and in π^+-π^0 scattering the exchange is present and all interactions may contribute.

However, although we have already considered the direct interaction between hadrons in a study of the simpler nonrelativistic quark model,[5] we prefer to postpone the study of the extremely interesting effects of quark exchange and direct interaction between two mesons.

Our aim, in this work, is to study the spectroscopy of resonances. Their energy is the sum of the eigenvalue of the Salpeter equation (that we call bare mass) plus a large complex energy shift. This shift comes from the coupling to open channels of two mesons. The effect of the direct meson-meson interactions in the two-meson channel is to add a potential term to the free energies of the mesons. The RGM equations now take the form

$$\begin{bmatrix} E-E_c & -i\langle v_{12}| \\ -i|v_{21}\rangle & E-E_a-E_b-V_2 \end{bmatrix} \begin{bmatrix} c_1 \\ |\chi_2\rangle \end{bmatrix} = 0 , \qquad (3.32)$$

where the potential V_2 is a separable potential that is calculated with an overlap of the bare meson wave functions and the interaction. For resonances this shift of the cut in the 22 channel only corresponds to a background that will distort the energy shift of the resonance. In the case of the ϕ we do not expect this background to be important because few diagrams contribute to it. In the case of the ρ we expect the background to have a bigger influence. In any case, many cancellations occur in the calculation of the background, and we do not expect it to distort greatly the contribution of the free energy of the two mesons to the pole of the resonance.

IV. s- AND t-MATRIX FORMALISM WITH A SEPARABLE POTENTIAL

The s matrix can take the form

$$\begin{bmatrix} s_{11} & s_{12} \\ s_{21} & s_{22} \end{bmatrix} = \frac{i}{\begin{bmatrix} E-E_c+i\epsilon & -i\langle v_{12}| \\ -i|v_{21}\rangle & E-E_a-E_b+i\epsilon \end{bmatrix}} \qquad (4.1)$$

but the s_{ij} matrices are simpler to determine directly from the following relations. From (3.27), we get

$$s_{11} = \frac{1}{1-g_1\langle v_{12}|g_2|v_{21}\rangle} g_1 = \frac{1}{E-E_c-\left\langle v_{12}\left|\frac{1}{E-E_a-E_b+i\epsilon}\right|v_{21}\right\rangle + i\epsilon} . \qquad (4.2)$$

As s_{11} is a matrix in the space generated by the eigenstates of Salpeter equations, it has poles at the zeros of the determinant:

$$\det\left[(E-E_c)\delta_{cc'} - \sum_{a=1,\ b=1}^{n_a,n_b} \left\langle v_{12_{cab}}\left|\frac{1}{E-E_a-E_b+i\epsilon}\right|v_{21_{abc}}\right\rangle\right] . \qquad (4.3)$$

If we consider a single bound state or resonance ($n_c=1$) then the pole lies at

$$E_r - i\frac{\Gamma}{2} = E_1 + \sum_{a=1,\ b=1}^{n_a,n_b} \left\langle v_{12_{lab}}\left|\frac{1}{E-E_a-E_b+i\epsilon}\right|v_{21_{ab1}}\right\rangle . \qquad (4.4)$$

Now, iterating (3.24), we obtain for s_{22},

$$s_{22} = g_2 + g_2|v_{21}\rangle s_{11}\langle v_{12}|g_2 . \qquad (4.5)$$

As for s_{12} and s_{21} we have directly from (3.26a) and (3.26b) that

$$s_{12} = s_{11}\langle v_{12}|g_2, \quad s_{21} = g_2|v_{21}\rangle s_{11} . \qquad (4.6)$$

These results satisfy (3.30) where the pole is s_{11} itself, c_1 is identical to $\mathbb{1}$, and $|\chi_2\rangle$ is equal to $\langle v_{12}|g_2$,

According to (4.5) we can define the on-shell T matrix in the channel two to be (where p_2 is the relative momentum of the mesons A and B)

$$T_{2_{ab}} = \sum_c \langle p_2|v_{21_{abc}}\rangle s_{11_{cc}}\langle v_{12_{cab}}|p_2\rangle , \quad p_2 = \sqrt{(E/2)^2 - M^2} . \qquad (4.7)$$

Then the scattering amplitude, which gives the Argand plot is

$$A = -\frac{\pi}{4} p_2 E T_{2_{ab}} . \qquad (4.8)$$

V. ANNIHILATION OVERLAP IN P-WAVE MESON SCATTERING

In this section we proceed to the evaluation of the overlaps. First, and taking advantage of the instantaneous nature of the interaction, we integrate out the energies; and we define the truncated potentials. Next, we consider all the diagrams contributing to the overlap of these truncated potentials and evaluate them by steps. We will study in greater detail the $\langle K^+|\langle K^-|V_{21}|\phi\rangle$ overlap, and we will only show the results for the similar $\langle K_S|\langle K_1|V_{21}|\phi\rangle$ and $\langle \pi^+|\langle \pi^0|V_{21}|\rho^+\rangle$.

A. Truncated potentials: V_{12} and V_{21} truncated

In Fig. 8, we show a typical diagram responsible for the annihilation (creation) of two mesons in one. Only the energies flowing in the fermionic lines are represented. We postpone to the next paragraphs the discussion of the more complicated momentum dependence. This is possible due to the simplifying features of the instantaneous potentials. Not depending on energy[2] (except for the Dirac delta that conserves the total energy), they allow in turn, the Salpeter bound-state mesonic wave functions to be independent of the relative energy between the quarks. Therefore, we are able to integrate out the energies independently of the momenta. The contribution of the diagram of Fig. 8 reads

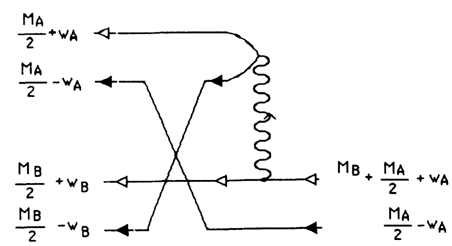

FIG. 8. Typical diagram, ultimately responsible for the formation or destruction of a resonance, in the scattering of two mesons. Only the energies flowing in the fermionic lines are displayed.

$$\mathbf{I}=\int \frac{dw_A dw_B}{(2\pi)^2}\frac{i}{\frac{M_A}{2}+w_A-E_q\left[+\frac{\mathbf{p}}{2}+\mathbf{k}\right]+i\epsilon}$$
$$\times\frac{i}{\frac{M_A}{2}-w_A-E_{\bar q}\left[+\frac{\mathbf{p}}{2}-\mathbf{k}\right]+i\epsilon}\frac{i}{\frac{M_B}{2}+w_B-E_q\left[-\frac{\mathbf{p}}{2}+\mathbf{k}'\right]+i\epsilon}$$
$$\times\frac{i}{\frac{M_B}{2}+w_B-E\bar{q}\left[-\frac{\mathbf{p}}{2}-\mathbf{k}'\right]+i\epsilon}\frac{i}{M_B+\frac{M_A}{2}-w_A-E_q\left[-\frac{\mathbf{p}}{2}+\mathbf{k}\right]+i\epsilon}\ . \tag{5.1}$$

Performing the integrations in w_A and w_B we get

$$\mathbf{I}=\frac{i}{M_A-E_q\left[+\frac{\mathbf{p}}{2}+\mathbf{k}\right]-E_{\bar q}\left[+\frac{\mathbf{p}}{2}-\mathbf{k}\right]+2i\epsilon}$$
$$\times\frac{i}{M_B-E_q\left[-\frac{\mathbf{p}}{2}+\mathbf{k}'\right]-E_{\bar q}\left[-\frac{\mathbf{p}}{2}-\mathbf{k}'\right]+2i\epsilon}\frac{i}{M_A+M_B-E_q\left[-\frac{\mathbf{p}}{2}+\mathbf{k}\right]-E_{\bar q}\left[\frac{\mathbf{p}}{2}-\mathbf{k}\right]+2i\epsilon}$$
$$=G_{A^0}(M_A)G_{B^0}(M_B)G_{C^0}(M_a+M_B)=G_2G_1\ , \tag{5.2}$$

where $\mathbf{k},\mathbf{k}'$ and $-\mathbf{p}/2+\mathbf{k}$ are, respectively, the momenta flowing inside mesons A, B, and C (see Fig. 8).

Although the integral only contains five quark propagators, we end up with the usual Green's functions G_1 and G_2 that correspond to the two incoming quarks and the four outgoing quarks. In this way we can factorize G_1 and G_2, and this allows us to use (3.21), where the one-meson S matrix includes all the propagators and the meson-meson interaction must be used in the truncated form.

All similar diagrams (see Fig. 9), when integrated over the energies, will yield the same result.

B. Evaluation of the truncated amplitudes $\langle\phi_A|\langle\phi_B|V_{21,\ \mathrm{truncated}}|\phi_1\rangle$

The Feynman diagrams contributing to (3.21) are shown in Fig. 9, except for the similar diagrams where quarks instead of antiquarks are exchanged. $A^{+,-}$, $B^{+,-}$, and $C^{+,-}$ stand for the wave functions of our three mesons. The superscript $+-$, represents, as usual, positive- and negative-energy components of the mesonic wave functions. As we have seen, explicit evaluation of the negative-energy components and D- wave components of the ϕ and of the ρ, shows that they are negligible.[3] In the figure, the quarks' momenta, flavor, and spin projections are also depicted. The energies flowing in the quark lines have been omitted. We will substitute for A, B, and C, the mesons $K^+(K_s,\pi^+)$, $K^-(K_l,\pi^0)$, and $\phi(\phi,\rho^+)$, to obtain the reactions we want to study.

We calculate the overlap with the same technique that we used in Ref. 3 for the derivation of Salpeter equation. Including the factor $-\frac{4}{3}$ that comes from the traces in color and is absorbed in the strength of the potential (we also use units of $K_0=1$), the minus sign that comes from the exchange, and the Laplacian that comes from the potential and the integration in $\mathbf{k}'$, we have to calculate the overlap:

$$
\begin{aligned}
\frac{-2\sqrt{2}}{\sqrt{3}}\int\frac{d^3k'}{(2\pi)^3}\sum_{s_1s_2s_3s_4s_5}\Bigg\{&\Phi^{+\dagger}_{A,s_1s_2}(\mathbf{k})u^\dagger_{s_1}\left[+\frac{\mathbf{p}}{2}+\mathbf{k}\right]\nabla_{\mathbf{k}'}v_{s_4}\left[+\frac{\mathbf{p}}{2}+\mathbf{k}'\right]\Phi^{+\dagger}_{B,s_3s_4}(\mathbf{k})\\
&\times\Bigg[-\nabla_{\mathbf{k}'}\Phi^{+}_{C,s_3s_2}\left[-\frac{\mathbf{p}}{2}+\mathbf{k}'\right]\\
&\quad+\nabla_{\mathbf{k}'}u^\dagger_{s_3}\left[-\frac{\mathbf{p}}{2}+\mathbf{k}'\right]u_{s_5}\left[-\frac{\mathbf{p}}{2}+\mathbf{k}\right]\Phi^{+}_{C,s_5s_2}\left[-\frac{\mathbf{p}}{2}+\mathbf{k}\right]\\
&\quad-\Phi^{+}_{C,s_3s_5}\left[-\frac{\mathbf{p}}{2}+\mathbf{k}\right]\nabla_{\mathbf{k}'}v^\dagger_{s_5}\left[-\frac{\mathbf{p}}{2}+\mathbf{k}'\right]v_{s_2}\left[-\frac{\mathbf{p}}{2}+\mathbf{k}\right]\Bigg]\\
&+\Phi^{+}_{C,s_3s_2}\left[-\frac{\mathbf{p}}{2}+\mathbf{k}\right]v^\dagger_{s_2}\left[-\frac{\mathbf{p}}{2}+\mathbf{k}'\right]\nabla_{\mathbf{k}'}u_{s_1}\left[-\frac{\mathbf{p}}{2}+\mathbf{k}'\right]\Phi^{-}_{A,s_1,s_4}(\mathbf{k})\\
&\times\Bigg[\nabla_{\mathbf{k}'}\Phi^{+\dagger}_{B,s_3s_4}(\mathbf{k}')+\Phi^{+\dagger}_{B,s_5s_4}(\mathbf{k})\nabla_{\mathbf{k}'}u^\dagger_{s_5}\left[-\frac{\mathbf{p}}{2}+\mathbf{k}'\right]u_{s_3}\left[-\frac{\mathbf{p}}{2}+\mathbf{k}\right]\\
&\quad-\nabla_{\mathbf{k}'}v^\dagger_{s_4}\left[+\frac{\mathbf{p}}{2}+\mathbf{k}'\right]v_{s_5}\left[+\frac{\mathbf{p}}{2}+\mathbf{k}\right]\Phi^{+\dagger}_{B,s_3s_5}(\mathbf{k})\Bigg]\\
&+\Phi^{-}_{B,s_1s_4}(\mathbf{k})v^\dagger_{s_4}\left[-\frac{\mathbf{p}}{2}+\mathbf{k}\right]\nabla_{\mathbf{k}'}u_{s_3}\left[-\frac{\mathbf{p}}{2}+\mathbf{k}'\right]\Phi^{+}_{C,s_3s_2}\left[-\frac{\mathbf{p}}{2}+\mathbf{k}\right]\\
&\times\Bigg[\nabla_{\mathbf{k}'}\Phi^{+\dagger}_{A,s_1s_2}(\mathbf{k}')+\Phi^{+\dagger}_{A,s_5s_2}(\mathbf{k})\nabla_{\mathbf{k}'}u^\dagger_{s_5}\left[+\frac{\mathbf{p}}{2}+\mathbf{k}'\right]u_{s_1}\left[+\frac{\mathbf{p}}{2}+\mathbf{k}\right]\\
&\quad-\nabla_{\mathbf{k}'}v^\dagger_{s_2}\left[-\frac{\mathbf{p}}{2}+\mathbf{k}'\right]v_{s_5}\left[-\frac{\mathbf{p}}{2}+\mathbf{k}\right]\Phi^{+\dagger}_{A,s_1s_5}(\mathbf{k})\Bigg]\Bigg\}\Bigg|_{\mathbf{k}'=\mathbf{k}}\,,
\end{aligned}
\tag{5.3}
$$

where we only write the nonvanishing terms (when u^+v, v^+u, or u^+u-v^+v are not derived, they vanish). In expression (5.3), u and v represent, as usual the Dirac spinors, whereas $\phi^{(+,-)}_{A,B,C}$ are the appropriate meson wave functions. The s_i's stand for the spin projections.

With our choice of coordinates, the spinors carrying $-\mathbf{p}/2$ correspond to s and $\bar{s}$ quarks while the ones with $\mathbf{p}/2$ correspond to u and $\bar{u}$ quarks. We also notice that the lines of the s quark connect the meson ϕ to one of the mesons K, while the u lines only connect K mesons.

1. Covariant approximation

Because our potential is not covariant, we have a consistency problem, when choosing for a given quark, the rest frame in which to solve the mass gap equation for the vacuum angle ϕ. We cannot choose a universal frame for the vacuum angle ϕ. A proper calculation should have started, from the onset, with a covariant potential. This, in itself, would constitute a formidable task in addition to the present, already involved, calculations. In the case of a universal rest frame, it was shown in Ref. 1 that a massless pion would have a speed approximately three times larger than the speed of light. We choose to make the assumption that to each quark there corresponds a vacuum angle centered on the center of mass of its parent meson. We hope that, with this assumption, our model becomes approximately covariant and, in this way, the potential in a meson depends only on the intracluster relative momen-

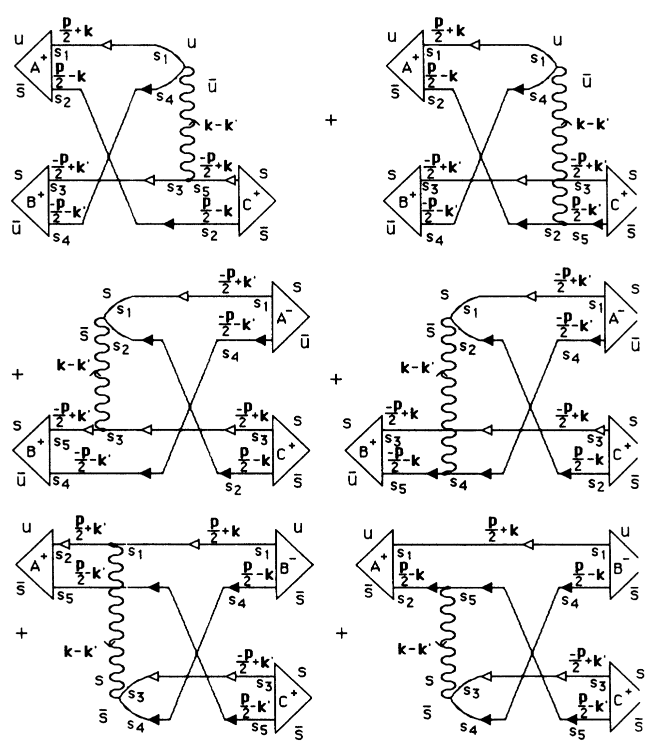

FIG. 9. Diagrams responsible for the formation (and destruction) of resonance C in the scattering of two meson: A and B. The diagrams displaying the contribution of the negative-energy components of the mesonic wave functions are also presented.

tum. Therefore we assume the following.

(1) The wave functions Φ_M can be approximated by those obtained in the center of mass of the meson. These were obtained in Ref. 3 and depend only on the intracluster relative momentum.

(2) The spinors for the quark u (here, only to be found in the K mesons) will depend only on the $q\bar{q}$ relative momentum inside the mesons. If we use the vacuum angle obtained in Ref. 2, then $(\mathbf{p}/2)+\mathbf{k}$ should be replaced by $\mathbf{k}$.

(3) The quark s (shared by K and ϕ mesons) has a relative momentum of $-(\mathbf{p}/2)+\mathbf{k}$ inside the meson ϕ and a relative momentum of $\mathbf{k}$ inside meson K. We take an average momentum frame for the s quarks and replace $-(\mathbf{p}/2)+\mathbf{k}$ by $-(\mathbf{p}/4)+\mathbf{k}$ in the respective spinors.

(4) The energy of a meson with total momentum $\mathbf{p}$ and mass M should be given by the usual expression $E_M=\sqrt{\mathbf{p}^2+M^2}$.

In any case, the results without using assumptions (2) and (3) will be also presented.

2. Spinor derivatives

We have to calculate the spinor derivatives are (see Refs. 2 and 3)

$$u_s^\dagger(\mathbf{k})\frac{\partial}{\partial k_a}[v_{s'}(\mathbf{k})]=\frac{1}{2}\left[\frac{C}{k}\mathbf{e}_a-\left[\varphi'+\frac{C}{k}\right]\frac{k_a\mathbf{k}}{k^2}\right]\cdot(\sigma i\sigma_2)_{ss'} \tag{5.4}$$

because $-C/k$ and φ' only differ in their vanishing tail, we obtain

$$u_s^\dagger(\mathbf{k})\frac{\partial}{\partial k_a}[v_{s'}(\mathbf{k})]\simeq\frac{1}{2}\left[\frac{C}{k}\mathbf{e}_a\right]\cdot(\sigma i\sigma_2)_{ss'}\;. \tag{5.5}$$

Similarly, we have

$$v_s^\dagger(\mathbf{k})\frac{\partial}{\partial k_a}[u_{s'}(\mathbf{k})]=-\left[u_s^\dagger(\mathbf{k})\frac{\partial}{\partial k_a}[v_{s'}(\mathbf{k})]\right]^*\;. \tag{5.6}$$

In (u^+u-v^+v), only the term without a delta in the spins will contribute. We have

$$\frac{\partial}{\partial k_a}[u_{s'}^\dagger(\mathbf{k})]u_s(\mathbf{k})=-\frac{1}{2}\left[\frac{1-S}{k^2}\right][i\sigma_{ss'}\times\mathbf{k})\cdot\mathbf{e}_a+\delta_{ss'}\cdots \tag{5.7}$$

and

$$-\frac{\partial}{\partial k_a}[v_{s'}^\dagger(\mathbf{k})]v_s(\mathbf{k})=-\left[\frac{\partial}{\partial k_a}[u_{s'}^\dagger(\mathbf{k})]u_s(\mathbf{k})\right]^*\;. \tag{5.8}$$

If mesons A and B have the same wave function in space and spin, the overlap (5.3) becomes

$$\begin{aligned}\frac{-2\sqrt{2}}{\sqrt{3}}\int\frac{d^3k}{(2\pi)^3}\Bigg[&\Phi_A^+(\mathbf{k})\Phi_A^+(\mathbf{k})\Phi_C^+\left[-\frac{\mathbf{p}}{2}+\mathbf{k}\right]\left[\frac{1}{2}\frac{C\left[\frac{\mathbf{p}}{2}+\mathbf{k}\right]}{\left|\frac{\mathbf{p}}{2}+\mathbf{k}\right|}\right]\left[+\frac{1}{\alpha_C^2}\right]\left[-\frac{\mathbf{p}}{2}+\mathbf{k}\right]\cdot\mathbf{t}_1\\
&+\Phi_A^+(\mathbf{k})\Phi_A^+(\mathbf{k})\Phi_C^+\left[-\frac{\mathbf{p}}{2}+\mathbf{k}\right]\left[\frac{1}{2}\frac{C\left[\frac{\mathbf{p}}{2}+\mathbf{k}\right]}{\left|\frac{\mathbf{p}}{2}+\mathbf{k}\right|}\right]\left[-\frac{1}{2}\frac{1-S\left[-\frac{\mathbf{p}}{2}-\mathbf{k}\right]}{\left|-\frac{\mathbf{p}}{2}+\mathbf{k}\right|^2}\right]\left[-\frac{\mathbf{p}}{2}+\mathbf{k}\right]\cdot\mathbf{t}_2\\
&+\Phi_A^+(\mathbf{k})\Phi_a^-(\mathbf{k})\Phi_C^+\left[-\frac{\mathbf{p}}{2}+\mathbf{k}\right]\left[\frac{1}{2}\frac{C\left[-\frac{\mathbf{p}}{2}+\mathbf{k}\right]}{\left|-\frac{\mathbf{p}}{2}+\mathbf{k}\right|}\right]\left[-\frac{1}{\alpha_A^2}\right]\mathbf{k}\cdot\mathbf{t}_3\\
&+\Phi_A^+(\mathbf{k})\Phi_A^-(\mathbf{k})\Phi_C^+\left[-\frac{\mathbf{p}}{2}+\mathbf{k}\right]\left[\frac{1}{2}\frac{C\left[-\frac{\mathbf{p}}{2}+\mathbf{k}\right]}{\left|-\frac{\mathbf{p}}{2}+\mathbf{k}\right|}\right]\left[-\frac{1}{2}\frac{1-S\left[-\frac{\mathbf{p}}{2}+\mathbf{k}\right]}{\left|-\frac{\mathbf{p}}{2}+\mathbf{k}\right|^2}\right]\left[-\frac{\mathbf{p}}{2}+\mathbf{k}\right]\cdot\mathbf{t}_4\\
&+\Phi_A^+(\mathbf{k})\Phi_A^-(\mathbf{k})\Phi_C^+\left[-\frac{\mathbf{p}}{2}+\mathbf{k}\right]\left[\frac{1}{2}\frac{C\left[-\frac{\mathbf{p}}{2}+\mathbf{k}\right]}{\left|-\frac{\mathbf{p}}{2}+\mathbf{k}\right|}\right]\left[-\frac{1}{2}\frac{1-S\left[\frac{\mathbf{p}}{2}+\mathbf{k}\right]}{\left|\frac{\mathbf{p}}{2}+\mathbf{k}\right|^2}\right]\left[\frac{\mathbf{p}}{2}+\mathbf{k}\right]\cdot t_5\Bigg]\;,\end{aligned} \tag{5.9}$$

where t_i are traces of the spin matrices, defined below.

3. Traces in spin

The spin wave functions of the positive-energy components are the following.

(1) For the K a spin singlet,

$$\Phi_A^+=\Phi_B^+=\frac{1}{\sqrt{2}}(\uparrow\downarrow-\downarrow\uparrow)=\frac{1}{\sqrt{2}}\begin{bmatrix}1 & 1\\ -1 & 0\end{bmatrix}=\frac{-i}{\sqrt{2}}\sigma_2 . \tag{5.10}$$

(2) For the ϕ, with spin 1, we choose the $\binom{1}{0}$ projection

$$\Phi_C^+=\frac{1}{\sqrt{2}}(\uparrow\downarrow+\downarrow\uparrow)=\frac{1}{\sqrt{2}}\begin{bmatrix}0 & 1\\ 1 & 0\end{bmatrix}=\frac{1}{\sqrt{2}}\sigma_1 . \tag{5.11}$$

We define the negative-energy wave functions to have the same spin wave functions. However in Ref. 3, we took the same spin wave functions for the negative-energy bras and the positive-energy kets. In fact we took

$$\Phi_M^+=\Phi_M^{-\dagger} , \tag{5.12}$$

where the adjoint sign † yields a minus sign for spin 0 and a plus sign for spin 1. If we adhere to the new convention,

$$\Phi_M^+=\Phi_M^- \tag{5.13}$$

then we must change, for the $^1S_0$ bound states (such as the K and the π), the sign of the space wave functions for the negative-energy terms that were obtained in Ref. 3.

Thus, for the new convention, the traces in spin indices are

$$\begin{aligned}
\mathbf{t}_1&=\mathrm{tr}(\Phi_A\sigma i\sigma_2\Phi_A\Phi_C)=\frac{1}{\sqrt{2}}\mathbf{e}_3 ,\\
\mathbf{t}_2&=\mathrm{tr}(\Phi_A\sigma i\sigma_2\Phi_A\times i\sigma\Phi_C\\
&\quad+\Phi_A\sigma i\sigma_2\Phi_A\Phi_C\times i\sigma^*)=-2\sqrt{2}\mathbf{e}_3 ,\\
\mathbf{t}_3&=\mathrm{tr}(\Phi_C\sigma^* i\sigma_2\Phi_A\Phi_A+\Phi_A\sigma^* i\sigma_2\Phi_C\Phi_A)\\
&=-\sqrt{2}\mathbf{e}_3 ,\\
\mathbf{t}_4&=\mathrm{tr}(\Phi_C\sigma^* i\sigma_2\Phi_A\Phi_A\times i\sigma\\
&\quad+\Phi_a\sigma^* i\sigma_2\Phi_C\times i\sigma^*\Phi_A)=2\sqrt{2}\mathbf{e}_3 ,\\
\mathbf{t}_5&=\mathrm{tr}(\Phi_A\sigma^* i\sigma_2\Phi_C\Phi_A\times i\sigma\\
&\quad+\Phi_C\sigma^* i\sigma_2\Phi_A\times i\sigma^*\Phi_A)=-2\sqrt{2}\mathbf{e}_3 .
\end{aligned} \tag{5.14}$$

4. Gaussian approximation of our functions

The wave functions are almost Gaussians. In Ref. 3 they were obtained numerically and their Gaussian approximation was given. With our new convention for the spin wave functions, we have to be careful to take both ϕ^+ and ϕ^- positive.

The functions C/k and $(1-S)/k^2$ also have a Gaussian shape except that their tail decays more slowly (like $1/k$ and $1/k^2$. However the tail is of little importance in the integral because it is multiplied by Gaussian tails. In this case, for numerical expediency, we can also approximate these functions by Gaussians. However, we cannot approximate them with a Gaussian with the same initial value and norm, as we did for the wave functions. Instead we impose the condition that the Gaussian coincides at the origin and at another point (at 1/3 of its height). This gives a good overall fit.

Then we just have to evaluate Gaussian integrals of the form

$$-2\int\frac{d^2k}{(2\pi)^3}\left[\mathbf{k}+\epsilon\frac{\mathbf{p}}{2}\right]\exp-\left[Ak^2+2B\mathbf{k}\cdot\frac{\mathbf{p}}{2}+C\left[\frac{\mathbf{p}}{2}\right]^2\right]=-\frac{\epsilon-B/A}{(4\pi A)^{3/2}}\mathbf{p}\exp\left[-\frac{1}{2}p^2\left[\frac{AC-BB}{2A}\right]\right] . \tag{5.15}$$

Except for the factor $\mathbf{p}$, we obtain a sum of five Gaussians with similar widths, which can be well approximated by a Gaussian. Then the final overlap is proportional to a harmonic-oscillator wave function with one angular excitation:

$$\phi_{010}^{\alpha}(\mathbf{p})=\left[\frac{2^4\pi^{3/2}}{\alpha^5}\right]^{1/2}p_3\exp\left[-\frac{p^2}{2\alpha^2}\right] . \tag{5.16}$$

5. Separable solution

The overlap (5.3) takes a separable form, where the left form factor is an harmonic-oscillator wave function of the K^+K^- relative momentum $\mathbf{p}$, and the right form factor is a c number:

$$|v_{21}\rangle=\mathcal{V}|\phi_{010}^{\alpha}\rangle . \tag{5.17}$$

The overlap of the ϕ with K_SK_L is, to a very good approximation, the same because a change of the quark u to the quark d is, in this case, quantitatively unimportant.

The ρ^+ can only decay to the single channel of $\pi^+\pi^0$, but the flavor overlap is larger by a factor of $\sqrt{2}$. As these overlaps are squared in the effective potentials, the flavor contribution happens to be equivalent for these two resonances. The differences between the respective overlaps are thus purely dynamical.

The overlap is a function of the parameters of our model (which are the strength of the potential K_0 and the current quark masses $m_u,m_d,m_s,\ldots$). Only one parameter remains free if we require our model to reproduce the physical masses of the pseudoscalar mesons (see Ref. 3):

$$\begin{aligned}
m_u&=\frac{1}{2K_0}\left[+\frac{m_K^{+2}}{c_K}-\frac{m_K^{02}}{c_K}+\frac{m_\pi^{+2}}{c_\pi}\right] ,\\
m_d&=\frac{1}{2K_0}\left[-\frac{m_K^{+2}}{c_K}+\frac{m_K^{02}}{c_K}+\frac{m_\pi^{+2}}{c_\pi}\right] ,\\
m_s&=\frac{1}{2K_0}\left[+\frac{m_K^{+2}}{c_K}+\frac{m_K^{02}}{c_K}-\frac{m_\pi^{+2}}{c_\pi}\right] ,
\end{aligned} \tag{5.18}$$

The above relations are the same as the Gell-Mann relations,[6,3] except that the constants c_π and c_K are slightly different because m_K and m_π are finite:

$$c_\pi = 17.14\ldots, \quad c_K = 15.10\ldots . \tag{5.19}$$

We choose the free parameter to be the strength of the potential K_0. Like all the parameters and wave functions, the annihilation overlaps are functions of K_0. In the case of the ϕ to K^+K^- or K_SK_L decay and of the ρ^+ to $\pi^+\pi^0$ decay we obtain the results of Table I.

VI. MATRIX ELEMENTS OF GREEN'S FUNCTIONS

With a separable potential, the T and S matrices are functions of the matrix elements of the free Green's function:

$$\left\langle \phi_{010}^{\alpha} \left| \frac{1}{E+i\epsilon-E_A-E_B} \right| \phi_{010}^{\alpha} \right\rangle = \frac{8}{3\sqrt{\pi}\alpha^5}\int_0^\infty dk \frac{k^4 e^{-k^2/\alpha^2}}{E+i\epsilon-2\sqrt{k^2+m^2}} \tag{6.1}$$

that has a complex pole at

$$p = \left[\frac{E^2}{4}-m^2\right]^{1/2} + i\epsilon$$

so that the overlap is given by

$$-\frac{2}{3\sqrt{\pi}\alpha^5}\int_0^\infty dk \frac{1}{k-\left[\left[\frac{E^2}{4}-m^2\right]^{1/2}+i\varepsilon\right]} \times \left[\frac{E+2\sqrt{k^2+m^2}}{k+\left[\frac{E^2}{4}-m^2\right]^{1/2}} k^4 e^{-k^2/\alpha^2}\right] . \tag{6.2}$$

When $E<2m$ the pole is not met by the integral. The integral is real and can be directly calculated.

When $E>2m$, we can calculate this overlap by decomposing it in two integrals:

$$\left\langle \phi_{010}^{\alpha} \left| \frac{1}{E+i\epsilon-E_A-E_B} \right| \phi_{010}^{\alpha} \right\rangle = I_1 + I_2 , \tag{6.3}$$

where I_1 is the principal value of the integral and I_2 is an integral in the complex plane. (See Fig. 10.) The real integral I_1 is easily determined numerically. It is convenient to decompose it in two terms:

TABLE I. The size α amplitude $\mathcal{V}$ of the creation overlap [see Eq. (5.17)] is given for the decay of ϕ to K^+K^- or K_SK_L and the decay of ρ^+ to $\pi^+\pi^0$. The overlap for ρ is larger than for the ϕ by a factor around 1.6 (in excess of the $\sqrt{2}$ that comes from the flavor). Because the contribution of the negative-energy components almost cancel numerically, the main reason behind this result is that the normalization of the positive-energy components of the π wave functions is almost double the normalization of the K positive-energy wave functions. Had we not taken the covariant assumption and maintained the full $\mathbf{p}/2$ dependence in the spinors, then $\mathcal{V}$ would be typically larger by a factor 3/2 and α would be smaller by a factor of 2/3. We will fix K_0 by reproducing the energy and width of the ρ and ϕ resonances. As the energy shifts are proportional to $\mathcal{V}^2$ and the imaginary energy shift is in first-order proportional to α^{-5}, it is clear that this would overestimate the results by an order of magnitude. This also shows that mesonic decays constitute an extremely sensitive test for our model.

Resonance	ϕ		ρ	
K_0	$\mathcal{V}$	α	$\mathcal{V}$	α
350	168	618	440	571
360	176	634	458	587
370	184	648	475	603
380	193	663	492	620
390	202	678	509	635
400	209	694	527	652
410	218	709	544	668
420	226	724	562	684
430	235	739	580	700
440	244	754	598	717
450	252	770	616	733
460	261	785	633	749
470	270	801	651	766
480	279	816	668	781
490	288	831	687	797
500	298	848	705	814
510	307	863	723	830
520	315	878	741	846
530	323	894	759	862
540	335	910	777	879
550	344	925	795	895

$$I_1 = -\frac{2}{3\sqrt{\pi}\alpha^5}\int_0^{2p} dk \frac{1}{k-p}\left[\frac{E+2\sqrt{k^2+m^2}}{k+p}k^4 e^{-k^2/\alpha^2} - Ep^3 e^{-p^2/\alpha^2}\right] + \frac{8}{3\sqrt{\pi}\alpha^5}\int_{2p}^\infty dk \frac{k^4 e^{-k^2/\alpha^2}}{E+i\epsilon-2\sqrt{k^2+m^2}} , \tag{6.4}$$

where the term $-Ep^3\exp(-p^2/\alpha^2)$, which has a vanishing principal value in the first term, was added to remove the pole of the integrand.

Because the integrand is a real and analytical function, the complex integral I_2 is exactly $i\pi$ times the residue (half of the result for a complete contour of the pole)

$$I_2 = -i\frac{2\sqrt{\pi}Ep^3}{3\alpha^5}e^{-p^2/\alpha^2} . \tag{6.5}$$

The integral is only complex when p is real ($E>2m$). In this way, the bound states only get an effective imaginary mass (and become a resonance) when the coupled channels of two bound states are above threshold. This method can, of course, be applied to any matrix element of the free Green's function in a compact form factor.

In the nonrelativistic limit of $E \simeq 2m$ and $\alpha \ll 2m$, we have approximately, in the main integration region,

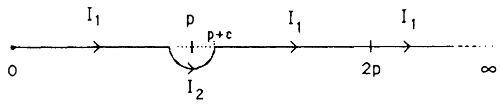

FIG. 10. Contours for the integrals I_1 and I_2.

$$2\sqrt{k^2+m^2} \simeq 2m + \frac{k^2}{m} \tag{6.6}$$

and the value of the integral can be obtained with the complex error function W:

$$I = -\frac{4m}{3\alpha^2}\left[\tfrac{1}{2}+Z^2+i\sqrt{\pi}Z^3W(Z)\right], \quad Z = \frac{\sqrt{m(E-2m)}}{\alpha} . \tag{6.7}$$

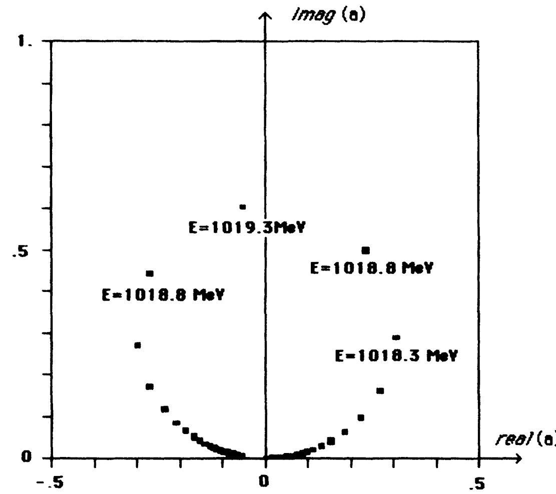

FIG. 11. Argand plot, given by our model, for K^+K^- P-wave scattering in the neighborhood of ϕ resonance.

VII. RESULTS AND CONCLUSION

A. ϕ Resonance and K^+K^- p-wave scattering

Our results are good with $K_0=402.6$ MeV: We obtain with our model a real energy shift of -94 MeV in M_ϕ and

$$M_\phi = 1019 \text{ MeV}, \quad 2\frac{\Gamma_{\phi \text{ to } K^+K^-}}{2} = 1.32 \text{ MeV} , \qquad 2\frac{\Gamma_{\phi \text{ to} K_SK_L}}{2} = 0.86 \text{ MeV} . \tag{7.1}$$

As the imaginary energy shift $-i\Gamma/2$ is very sensitive to α [see Eqs. (4.4) and (6.5)], a shift of 19% in α reproduces well the experimental results[7]

$$M_\phi = 1019 \text{ MeV}, \quad \Gamma_{\phi \text{ to } K^+K^-} = 2.18 \text{ MeV} . \qquad \Gamma_{\phi \text{ to } K_SK_L} = 1.52 \text{ MeV} . \tag{7.2}$$

Also, we used drastic approximations to make the model more covariant, and a small combination with 15% of the noncovariant overlap would reproduce the correct results. Moreover, we did not consider direct K-K interactions, and a small K-K attractive potential of the order of 10 MeV would agree with experiments. In this way the experimental results are within the errors of our approximations.

In Fig. 11 we show the argand plot for K^+K^- p-wave scattering. The plot lies inside the unitarity circle because the channel K_SK_L is open. Note that this plot verifies the width of the ϕ that we obtained directly in the pole of the T matrix.

A potential strength $K_0=402.6$ MeV corresponds to the current quark masses of

$$m_u = 1.08 \text{ MeV}, \quad m_d = 1.74 \text{ MeV}, \quad m_s = 39.0 \text{ MeV} . \tag{7.3}$$

B. ρ resonance and $\pi^+\pi^-$ p-wave scattering

The experimental mass and width for the ρ are[7]

$$M_\rho = 770 \text{ MeV}, \quad \Gamma_\rho = 153 \text{ MeV} . \tag{7.4}$$

With the value of $K_0=402.6$ MeV that we obtained for the ϕ resonance, we obtain for ρ a real energy shift of -328 MeV and

$$M_\rho = 742 \text{ MeV}, \quad \Gamma_\rho = 146 \text{ MeV} \tag{7.5}$$

which are not far from the experimental results of (7.4). For ρ, the background coming from direct $\pi\pi$ interaction is probably larger than the background for ϕ. Also, our approximation of covariance is probably worse for π-π scattering than for K-K scattering. Thus we were not expecting such excellent results.

In Fig. 12 we show the argand plot for $\pi^+\pi^0$ p-wave scattering. We find that the argand plots for the resonances ρ (Fig. 11) and ϕ (Fig. 12) satisfy the relation[8]

$$\left.\frac{\delta(\arg(a))}{\delta(E)}\right|_{E=E_r} = \frac{2}{\Gamma} \tag{7.6}$$

which is correct for a Fermi-Breit resonance. This checks our method.

C. Conclusion

This paper, together with Refs. 2 and 3 are part of a project to understand some basic aspects of hadronic physics. Assuming a microscopic interaction for quarks, using the same Feynman rules at each stage, we successively solved the mass gap equation,[2] the Bethe-Salpeter equation[3] for the bare meson masses and, finally, the RGM equations controlling mesonic scattering and decay. Except for the current quark masses and the potential strength we have no free parameters. The main conclusions of this paper are summarized below.

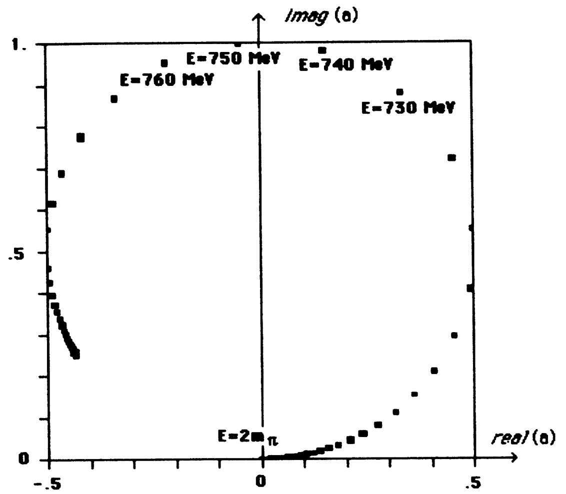

FIG. 12. Argand plot, given by our model, for $\pi^+\pi^0$ P-wave scattering in the neighborhood of ρ resonance.

It is inescapable that bare meson wave functions, i.e., prior to decay, have two components. This fact implies an essential departure from the Schrödinger equation. The lighter the current quarks, the higher the degeneracy between these two components. In the limit of massless current quarks, and for the case of pseudoscalar mesons, these two components are, with a possible difference of a phase, identical. The nonrelativistic limit is obtained when one of the components (in the text, the ϕ^-) tends to zero. In turn, the double component nature of the mesonic wave functions entails a quite specific normalization. Again in the limit of pseudoscalars with massless current quark masses, it is shown that the norm of each component diverges when the wave function is normalized to 1. This is a direct consequence of the degeneracy between the "positive-" and "negative-energy" components of the wave function. In particular we obtain that the norm of ϕ^+ for the π is almost double than the one for the K. This plays an essential role in the good results that we obtain for the decay of ρ and ϕ resonances.

For the potential adopted in this work, all the bare S-wave function components, "positive" and "negative energy," are very close to the Gaussian form. This allows us to use Gaussian wave functions when evaluating overlaps. The sizes of these Gaussians, the parameters α, depend directly on the size, in momentum space, of the region supporting the corresponding nonvanishing chiral angle. This is clearly seen in the case of the Goldstone pion wave function, that is simply given by the sine of the chiral angle.

The coupling of resonances with the corresponding mesonic asymptotic states is done in the framework of the RGM Schrödinger-type equation. But this does not involve any approximation other than the instantaneous approximation to the potential we use throughout this work. The RGM equations are the dynamical equations for coupled-channel systems of bound states and resonances. They are simply obtained when one substitutes, in the Dyson equations for the corresponding S matrix, the appropriate separable expansion in term of poles and the solutions[3] of the Bethe-Salpeter equation. In our case we recall that we have a condensed vacuum, with $^3P_0$ pairs, and relativistic quarks; the mesons have "positive-" and "negative-energy" components. Still the RGM equations are the correct equations to describe the decay of resonances into mesons, provided we use the correct expressions for the relativistic kinetic energy. Because the potential is confining, we find no explicit evidence of quarks in the final RGM equations, which seems to be correct in low-energy particle physics.

Apart from the implicit dependence of α on the chiral angle, this angle enters directly, through the microscopic vertices, into the evaluation of the overlap. Because of the ambiguity raised by the noncovariance of the adopted instantaneous potential, we were forced to make the assumption that to each quark there corresponds a vacuum (chiral) angle centered in the center of mass of its parent meson. Otherwise energy shifts between bare mesons and resonances would be too large.

We get, approximately, the right mass and width for the ρ, with the same parameter K_0 that gives the correct width for the ϕ (and fixes the quark masses). Taking into consideration the corresponding different chiral angles which are, themselves, functions of the current quark masses through the *nonlinear* mass gap equation, this gives us the assurance that this kind of model might have something to do with the real physical world.

The overlap potential, responsible for the annihilation (creation) of the two asymptotic mesons into (from) the resonance, depends quite heavily on the cluster sizes of the asymptotic mesons. This dependence of the imaginary part of the energy shift (the width of the resonance) going like α^{-5}. The real part of the energy shift is less sensitive to this parameter. It goes like α^{-3}. That we could get, simultaneously, sensible results for the ρ and ϕ, constitutes another source of confidence in models of this kind.

Our strange-quark masses, when compared with other values in the literature are smaller by a factor of 1/5. Presumably, covariance of the potential together with a more realistic form, of the type linear plus Coulomb, could improve on this value.

Adopting a covariant form for the potential and implementing at the same time a more realistic form for this potential are, we think, the prerequisites for a program towards the understanding of hadronic physics. It will be successful if it succeeds in explaining not only the wealth of data on hadronic masses, but also things such as the coupling of mesons to baryons, N-$\bar{N}$ scattering, and so on. We believe that, not withstanding the obvious shortcomings of the simple microscopic potential adopted in this work, many of the above conclusions will survive in a more realistic case. They show a picture quite different from the usual one given by the nonrelativistic quark model.

ACKNOWLEDGMENTS

We acknowledge the valuable comments and suggestions given to us by Vitor Vieira, George Rupp, and Antonio Amorim.

[1]A. Le Yaouanc, L. Oliver, O. Pène, J.-C. Raynal, and S. Ono, Phys. Rev. D **31**, 137 (1985).

[2]P. Bicudo and J. Ribeiro, preceding paper, Phys. Rev. D **42**, 1611 (1990).

[3]P. Bicudo and J. Ribeiro, preceding paper, Phys. Rev. D **42**, 1625 (1990).

[4]J. Wheeler, Phys. Rev. **52**, 1083 (1937); J. Ribeiro, Z. Phys. C **5**, 27 (1980).

[5]P. Bicudo and J. Ribeiro, Z. Phys. C **38**, 453 (1988).

[6]M. Gell-Mann, R. Oakes, and B. Renner, Phys. Rev. **175**, 2195 (1968).

[7]Particle Data Group, G. P. Yost *et al.*, Phys. Lett. B **204**, 1 (1988).

[8]R. Dalitz, in *Resonances—Models and Phenomena,* proceedings, Bielefeld, West Germany, 1984, edited by S. Albeverio, L. S. Ferreira, and L. Streit (Lecture Notes in Physics, No. 212) (Springer, Berlin, 1984), p. 1.